Available online at www.sciencedirect.com
ScienceDirect
Coordination Chemistry Reviews 250 (2006) 2491–2500
COORDINATION CHEMISTRY REVIEWS
www.elsevier.com/locate/ccr

Review

Enantioselective self-assembly of chiral bimetallic oxalate-based networks

Michel Gruselle [a,*], Cyrille Train [a], Kamal Boubekeur [a], Patrick Gredin [b], Nicholas Ovanesyan [c]

[a] *Laboratoire de Chimie Inorganique et Matériaux Moléculaires, UMR 7071, IFR 2769, Université Pierre et Marie Curie, case 42, 4 place Jussieu, F75252 Paris Cedex 05, France*
[b] *Laboratoire de Cristallochimie du Solide, UMR 7574, UPMC, case 176, 4 place Jussieu, F75252 Paris Cedex 05, France*
[c] *Institute of Problems of Chemical Physics, Russian Academy of Science, Moscow Region, 142432 Chernogolovka, Russia*

Received 17 November 2005; accepted 17 March 2006
Available online 2 May 2006

Contents

1. Introduction . . . 2491
2. Bimetallic oxalate-based networks: structures and control of the dimensionality . . . 2492
3. Three-dimensional networks . . . 2494
    3.1. Homochirality and tridimensionality . . . 2494
    3.2. From spontaneous resolution to enantioselective self-assembly of powdered and crystalline compounds . . . 2494
4. Two-dimensional bimetallic networks . . . 2495
    4.1. Heterochirality and bidimensionality . . . 2495
    4.2. Spontaneous resolution . . . 2497
    4.3. Enantioselective self-assembly of powdered samples . . . 2497
5. Summary . . . 2499
Acknowledgements . . . 2499
References . . . 2499

Abstract

Materials where two distinct physical properties coexist and may interact within one crystal lattice are a major target for molecular chemists. This review describes recent attempts towards oxalate-based chiral magnets in their optically active forms insisting on the possible control of both dimensionality and absolute configuration by supra-molecular self-assembly.

Keywords: Enantioselective self-assembly; Crystal engineering; Optically active magnets

1. Introduction

Synthesising multifunctional materials is a major trend in inorganic chemistry in general [1] and in molecular magnetism in particular [2,3]. Since the first experimental evidence for the magneto-chiral dichroic effect by physicists [4], efforts to obtain molecular materials exhibiting both long-range magnetic ordering and optical activity have been rapidly increasing [5,6]. In such materials, the magnetism is associated with unpaired electrons while chirality can be ligand-centered [5] or associated with tris(chelated) metal centres [6]. For both magnetism and optical activity, it is important to exert control both at the molecular and supramolecular levels. For the former, Kahn's model has shown to be a milestone to analyse and forecast the exchange interaction between two metal ions bridged by a diamagnetic ligand [7]. The control over chirality has not reached such a conceptual maturity yet, though theoretical tools to analyse quantitatively the chirality of transition metal complexes have recently been proposed [8]. From a synthetic point of view, two general strategies are developed to reach optically active coordination compounds:

- enantioselective synthesis or resolution of chiral ligands, transfer of chirality to the metal ion and control of its configuration through coordination bonds [9].

---

[*] Corresponding author. Tel.: +33 144273083; fax: +33 144273841.
E-mail address: gruselle@ccr.jussieu.fr (M. Gruselle).

doi:10.1016/j.ccr.2006.03.020

- chiral inductive effect of resolved building blocks in the formation of supramolecular structures [10].

The results presented and discussed here are relevant towards the second strategy applied to three- (3D) and two-dimensional (2D) oxalate-based bimetallic networks. This scope will focus on the main factors that control the enantioselective self-assembly leading to chiral 3D or 2D bimetallic oxalate-bridged networks in their optically active forms. A general presentation of these compounds will recall their structure and the conditions needed for their synthesis and the control of the dimensionality. For this review, the central characteristic of these compounds is related to their chirality. The next two sections will be devoted to the chirality and the possible control over configuration of the tris(chelated)metal centres first in 3D compounds then in 2D ones. Particular attention will be paid to the description of the relative configuration of the chiral centers in the anionic networks as well as, when needed, those of the counter-cations. Optically active compounds can sometimes be obtained by spontaneous resolution. Such a process cannot be considered as a preparative way because the control over absolute configuration is lost. Nevertheless conglomerates obtained by spontaneous resolution [11] will be described because understanding their synthesis is an important source of information concerning the chirality aspects of the self-assembly. It will be exploited as such before presenting the results obtained by enantioselective self-assembly.

2. Bimetallic oxalate-based networks: structures and control of the dimensionality

Oxalate is a widely used ligand in molecular magnetism. In 1992, Okawa et al. [12,13] described the synthesis of a series of ferromagnets of general formula $NBu_4[M^{II}Cr^{III}(ox)_3]$ (Bu = n-C_4H_9; M = Mn^{2+}, Fe^{2+}, Ni^{2+}, Cu^{2+}; ox = $C_2O_4{}^{2-}$) which was rapidly extended to many other metal ions pairs leading to para-, (canted) antiferro-, ferri- and ferromagnetic materials [14–16]. In contrast with the predictions of Okawa et al. [12], the structure of $NBu_4[MnCr(ox)_3]$ appeared to be composed of 2D $[M^{II}Cr^{III}(ox)_3]^-$ anionic layers [14,17,18]. The second crucial breakthrough was brought out by Decurtins et al. when they described analogous anionic networks with a 3D structure [15]. The question of the control of the dimensionality then pertinently arose. Previous reviews [2,3,19] have already tackled this problem but new intriguing results [20–23] deserve to be discussed and tentatively introduced in the general scheme of the control of dimensionality in oxalate-based compounds.

As demonstrated by Decurtins et al. [15], the structure of 3D oxalate-based compounds consists in a 10-gon 3-connected (10,3) anionic network (Fig. 1): the tris(oxalato)metalate moiety behaves as a 3-connector and the metal ions are located at the 10 summits of a decagon. This topological description can be viewed as three sets of interconnected helices of identical helicity (Fig. 2). A closer look at the structure revealed that the anionic network defines cavities of D_3 symmetry which welcome the counter-cations which also organise in a helicoidal manner. This occurrence has determined

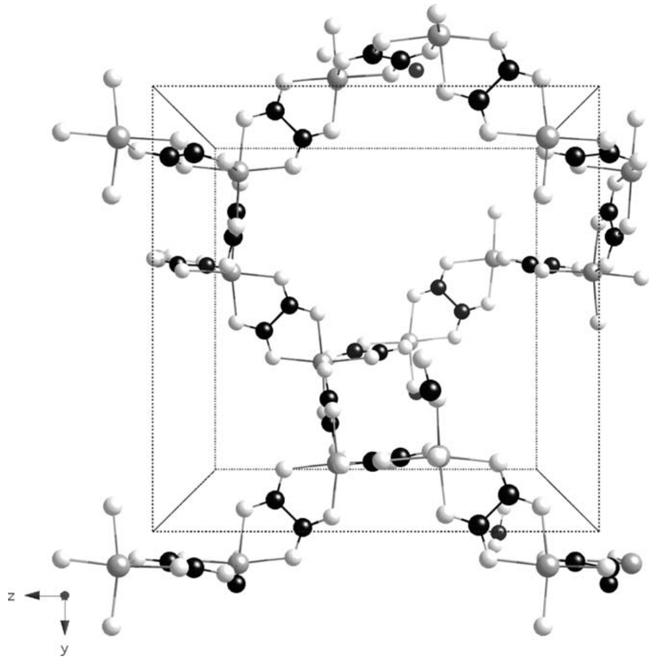

Fig. 1. 3D (10,3) anionic $[MM(ox)_3]^-$ network (drawn from the crystal data of Ref. [15]).

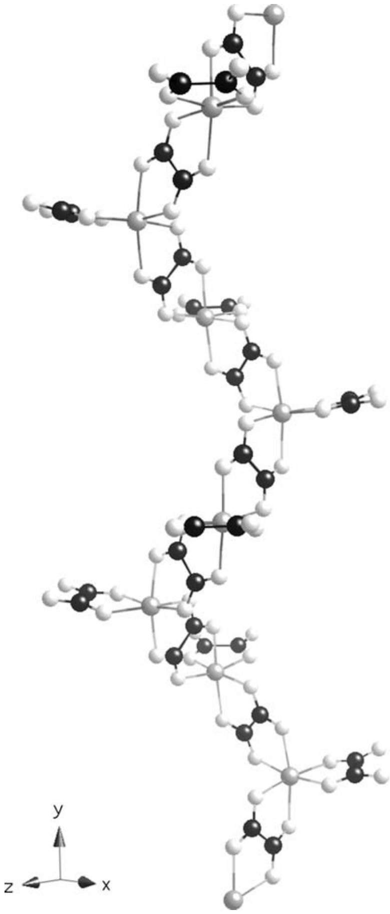

Fig. 2. Helix along the b-axis in the 3D compound $[\Lambda\text{-}Ru(bpy)_2(ppy)][\Lambda\text{-}Mn\Lambda\text{-}Cr(ox)_3]$ (drawn from the crystal data of Ref. [39]).

the most commonly used self-assembly pathway towards 3D oxalate-based networks. It is based on the use of D_3 symmetry tris(diimine)metal(II) complexes as template cations. Initially associated with tris(oxalato)metalates building blocks, these complexes have been exploited to synthesise new 3D compounds starting from the template cation combined with free oxalate and "naked" metal ions [6,15,24]. The anionic network is then built by successive wrapping of oxalate and metal ions around the D_3 template cations. From a magnetic point of view, $[\mathrm{M^{I}M^{III}(ox)_3}]^{2-}$ and $[\mathrm{M^{II}_2(ox)_3}]^{2-}$ anionic networks are essentially para- and/or antiferro-magnets. As described with 2D compounds [12,25], $[\mathrm{M^{II}M^{III}(ox)_3}]^{-}$ networks exhibit very rich and interesting magnetic properties. To obtain 3D $[\mathrm{M^{II}M^{III}(ox)_3}]^{-}$ networks, the cationic counterpart should bear only one positive charge. Taking into account the symmetry requirements underlined above, this can be provided either by a $[\mathrm{Ru^{II}(bpy)_3}]^{2+}$ (bpy = 2,2′-bipyridine) dication associated with a monoanion like $\mathrm{ClO_4}^-$ [6,26] or, more aesthetically (!), by the monocation bis(bipyridine)(phenylpyridine)ruthenium(II), $[\mathrm{Ru(bpy)_2(ppy)}]^+$ (ppy = 2-phenylpyridine) first described by Constable and Holmes [27] where the necessary negative charge is formally borne by the phenylpyridine ligand [6,28]. All these results highlight the strong templating effect of the tris(diimine)metal(II) complexes. Nevertheless, in some cases, this vision of the synthetic process appears oversimplified. For example, using tris(1,10-phenantroline)iron(II) as template cation, Armentano et al. obtained, together with the $[\mathrm{Fe(phen)_3}][\mathrm{NaFe(ox)_3}]$ (phen = 1,10-phenantroline) 3D compound, a 1D compound of formula $[\mathrm{Fe(phen)_3}]$-$[\mathrm{NaFe(ox)_3(H_2O)_3}]\cdot 4\mathrm{H_2O}$ [22]. This result reminds us that although tris(diimine)metal complexes are able to impose a tris-bischelated environment to metal ions that scarcely show such geometry [24,29], they sometimes partly failed in their templating activity. In the present case, iron(III) ends up in a D_3 environment, surrounded by three bis(chelating) oxalate ligands but, due to the versatility of its chemistry, sodium(I) is in a much more distorted environment, preventing the formation of the 3D network.

The structure of $\mathrm{NBu_4[MnCr(ox)_3]}$, first established by Atovmyan et al. [14], revealed that the main feature of this compound is a 2D honeycomb anionic network (Fig. 3a). For direct comparison with 3D compounds, an anionic layer can be described as a 6-gon 3-connected (6,3) anionic network: the tris(oxalato)metalate moiety still behaves as a 3-connector but the metal ions are now located at the six summits of a hexagon.

The tetra(butyl)ammonium cations are located between the anionic layers in such a way that each $\mathrm{NBu_4}$ stands on the three-fold symmetry axis above "$\mathrm{Cr(ox)_3}$" moieties only. One of the butyl chains penetrates the honeycomb cell of the upper layer (Fig. 3b). It is orientationally disordered around the three-fold axis, i.e. there are three equivalent conformations of this hydrocarbon chain. The three remaining butyl chains are located in the interlayer space. They stretch above the oxygen atoms of the three oxalates of the underlying "$\mathrm{Cr(ox)_3}$" moiety (Fig. 3a). Quaternary ammonium possessing four identical hydrocarbon chains with less than three carbon atoms do not lead to a formation of infinite networks. On the contrary, with ammonium ions with four different alkyl chains, one of the alkyl chains can be a mere methyl group [30,31].

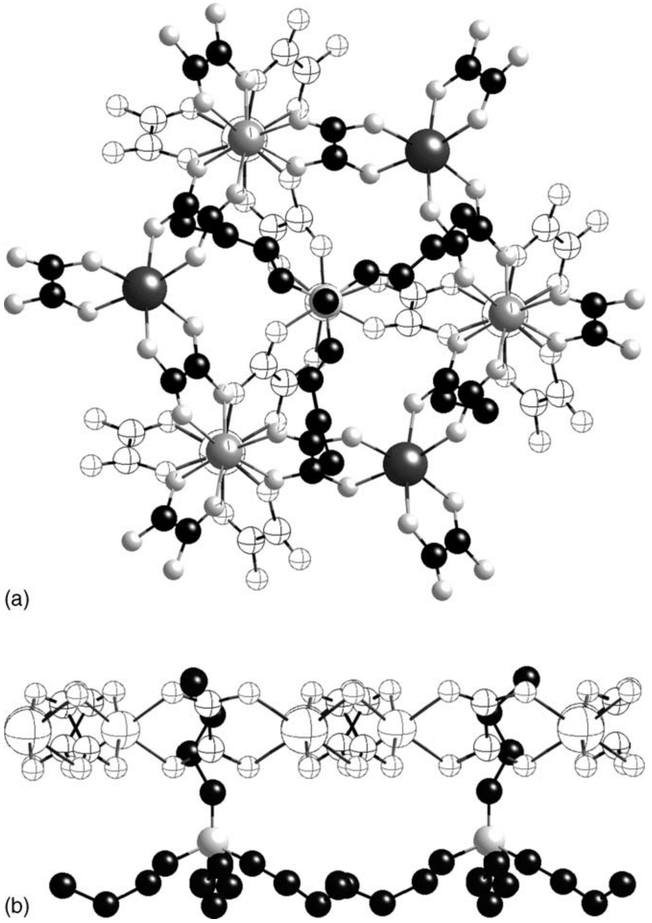

Fig. 3. Views of the 2D $[\mathrm{NBu_4}][\mathrm{MnCr(ox)_3}]$ compound perpendicular to the *c* axis (in sake of clarity, only the first carbon atom of the axial alkyl chain of the $[\mathrm{N}(n\text{-}\mathrm{C_4H_9})_4]^+$ cation is shown and the lower and upper anionic layers are differently represented) (a) along the *c* axis (b) (drawn from the crystal data of Ref. [14]).

In contrast with the 3D networks, it appears much more complicated to determine the necessary conditions to be fulfilled by the counter-cations to allow the formation of 2D networks. These uncertainties make the 2D anionic network an ideal framework for a wide range of counter-cations. This versatility has been exploited to replace the electronically innocent, diamagnetic ammonium ions by functional ones [3]: paramagnetic [32], photochromic [33], NLO active [34], charge-transfer donors [35], etc. The resulting materials are therefore bifunctional (dual acting) molecular magnets. In all cases mentioned in the literature, due to the ordered arrangement of the cations in the structure, the crystal symmetry was much lower than for highly symmetric tetraalkylammonium ions. Strong deviations from ideal honeycomb structure of the bimetallic layers are then the signature of an intermolecular interaction between the organic cations and the anionic framework. Nevertheless, in contrast with the situation observed in 3D compounds, the templating activity of the counter-cation is not sufficient to create in situ "$\mathrm{M(ox)_3}$" moieties: 2D compounds must be synthesised starting from tris(oxalato)metalate building blocks. A noticeable exception to the orientation of the synthesis towards 2D networks was reported by Alberola et al. [23] Pyridinium substituted nitronyl-nitroxide radical templated the formation of a 3D $[MnCr(ox)_3(H_2O)]^-$ anionic network. This result should be compared to the case of $[Fe(phen)_3][NaFe(ox)_3(H_2O)_3]\cdot 4H_2O$ described above [22]. In the present case, the manganese(II) ion is surrounded by two bis(chelating) oxalate ligands, one monodentate oxalate ligand and one water molecule. Once again, this unexpected coordination mode of the oxalate modifies the connecting rules between the different moieties and hence the topology of the network.

To finish with, special attention will be paid to the case of PPh_4^+ (Ph = C_6H_5) and PPh_3R^+ where R is an aliphatic alkyl chain. In accordance with their point group symmetry, which is different from D_3, these cations lead to 2D networks. This is indeed the result obtained for bimetallic networks consisting of one divalent and one trivalent transition metal ion [17,36,37]. Compared with quaternary ammonium ions, because of the rigidity of the phenyl group, $[PPh_4]^+$ is less disordered in the 2D compounds since two thirds of the axial phenyl groups have a rigid orientation while the remaining third are orientationally disordered. In contrast with the (M^{II}, M^{III}) case, for (M^{II}, M^{II}) or (M^{I}, M^{III}) pairs, PPh_4^+ [21] and PPh_3Me^+ [20] cations lead to the formation of 3D (10,3) anionic networks. In these cases, the counter-cations just act as a tris(chelated) template cation like $[M^{II}(bpy)_3]^{2+}$! Following calculations of the intermolecular interactions developed by Russell et al. [20], three reasons can be put forward to justify why non-D_3 cations appear to be able to build up 3D networks with the (10,3) topology:

(i) The enhanced charge of the anionic network imposes the presence of two mono-cations to compensate its charge. Contrasting with the case of $[M(bpy)_3]^{2+}$ cations, the mean distance reduction between the $[PPh_3Me]^+$ cations allows supramolecular interactions.
(ii) These are such that, despite their symmetry, the phosphonium cations behave as 3-connectors and form a (10,3) supramolecular cationic network which interpenetrates the (10,3) anionic network.
(iii) This interlacing allows stronger offset face-to-face interactions between the oxalate and the phenyl groups leading to a stabilisation of the 3D structure compared to the 2D one.

The examples reported in the literature highlight the usefulness of phenomenological and topological approaches based on simple symmetry arguments to control the dimensionality of extended networks. The case reported by Russell et al. [20] underlines the importance, for borderline cases, to take into account quantitatively all the supramolecular interactions to fully understand the observed topologies and go further into the forecast of self-assembled structures.

In both 3D and 2D oxalate-based compounds we will focus on in the following sections, *all* the metal centres of the anionic networks are tris(chelated) (as stressed above, if this condition is not fulfilled, the topology of the compound is much more versatile and difficult to predict). Such metal centres exhibit propeller-like chirality (Fig. 4) and, as pointed out below, the relative configurations of the metal centres are closely related to the dimensionality of the compound. The control over absolute configuration then appears as the second key point to be understood in these materials.

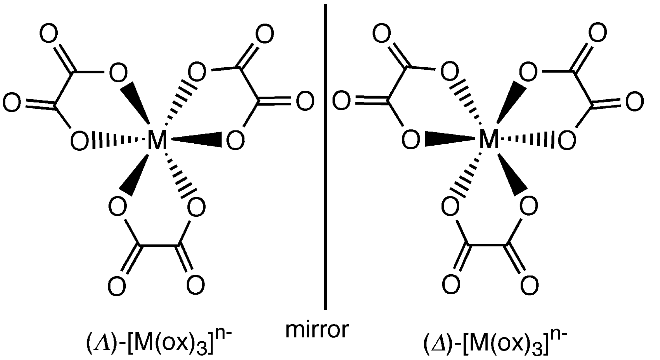

Fig. 4. Schematic views of the (Δ) and (Λ) enantiomers of $[Cr(ox)_3]^{3-}$.

3. Three-dimensional networks

3.1. Homochirality and tridimensionality

In 3D compounds, all the metal centres of the anionic network exhibit the same configuration (Fig. 5). Anionic helices of M or P absolute configuration, are exclusively built up by tris(chelated) metal centres of Δ or Λ configuration, respectively. Such inorganic helices can be compared with DNA helices, which in nature are exclusively built up by D-nucleotides. As sketched by Hargittai and Hargittai (Ref. [38, p. 74]), this homochirality is a necessary condition for building helices.

When the 3D anionic networks is formed by using a tris(diimine)metal complex, the configuration of the template cation is the same as that of the oxalate-bridged tris(chelated) metal ions. Such an arrangement favors the offset face-to-face interaction between the anionic network and the cationic counterpart [20]. For a homometallic $[M^{II}_2(ox)_3]^{2-}$ anionic network, the enantiomorphic space group of the crystals is $P4_132$ (respectively $P4_332$) when the metal centres adopt the Λ (respectively Δ) configuration [39]. For a heterometallic $[MM^{III}(ox)_3]^{n-}$ anionic network, the space group of the crystals is $P2_13$ for both configurations but the crystals definitely present different helicities as characterised by their Flack parameter depending on the configuration of the tris(chelated)metal centres [40].

As far as enantioselective self-assembly is concerned, the homochiral arrangement of all the coordinated metal centres is the most important feature of these 3D (10,3) structures.

3.2. From spontaneous resolution to enantioselective self-assembly of powdered and crystalline compounds

Decurtins et al. soon recognised the homochirality of all the coordinated metal centres as the driving force of the spontaneous resolution process occurring in these materials [15]. Using the chiral recognition between the template cation and the anionic building blocks, they produce chiral single crystals of either helicity. Nevertheless the crystals obtained starting from racemic

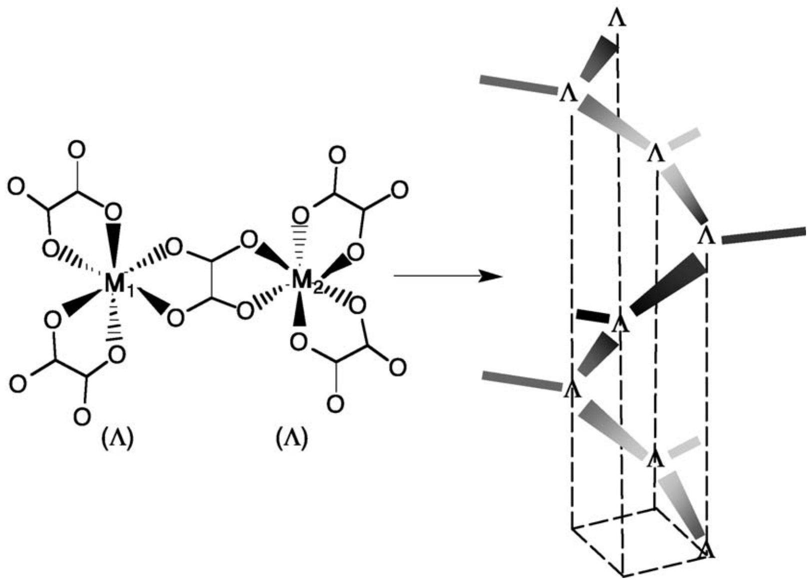

Fig. 5. Homochiral arrangement of the neighbouring tris(chelated) metal centres leads to a 3D (10,3) anionic network.

materials are often twinned. Moreover, a statistical assembly of crystals, called a racemic conglomerate [11], or powdered samples obtained by this technique do not show any optical activity.

Two strategies have been developed to obtain optically active 3D compounds. They differ by the choice of the chiral inductors.

The first approach uses resolved tris(oxalato)metalates [39]. As demonstrated by natural circular dichroism (NCD), the enantioselective homochiral self-assembly of the 3D network then leads to the insertion of only one enantiomer of the template cation within the sample while the second one remains in solution, according to the following reaction schemes:

$$2(rac)\text{-}[\mathrm{Ru(bpy)_3}]^{2+} + \Delta\text{-}[\mathrm{Cr(ox)_3}]^{3-} + \mathrm{Li}^{+} = [\Delta\text{-}\mathrm{Ru(bpy)_3}][\Delta\text{-}\mathrm{Li}\Delta\text{-}\mathrm{Cr(ox)_3}] + \Lambda\text{-}[\mathrm{Ru(bpy)_3}]^{2+}$$

$$2(rac)\text{-}[\mathrm{Ru(bpy)_3}]^{2+} + \Lambda\text{-}[\mathrm{Cr(ox)_3}]^{3-} + \mathrm{Li}^{+} = [\Lambda\text{-}\mathrm{Ru(bpy)_3}][\Lambda\text{-}\mathrm{Li}\Lambda\text{-}\mathrm{Cr(ox)_3}] + \Delta\text{-}[\mathrm{Ru(bpy)_3}]^{2+}$$

It clearly appears that the choice of the starting enantiomer fully determines the configuration of *all* the coordinated metal centres in the final compound. This strategy is interesting to obtain the optically active materials themselves but it has also been exploited to achieve the resolution of $[\mathrm{Ru(bpy)_2(ppy)}]^{+}$ for which the classical “tartrate” route used for homoleptic tris(diimine)metal(II) complexes failed [41].

There are two drawbacks to this strategy:

- the rapid racemisation of tris(oxalato)metalate compared to crystal growth rate favors the formation of racemic conglomerates.
- it cannot be applied when the resolution of the tris(oxalato)metalate complexes is not possible or when the complex does not exist.

The backbone of the second strategy. uses resolved tris(diimine)metal(II) complexes [6,24,39]. The general reaction schemes are then the following:

$$\Delta\text{-}[\mathrm{M(bpy)_3}]^{2+} + 2\,(rac)\text{-}[\mathrm{Cr(ox)_3}]^{3-} + \mathrm{Li}^{+} = [\Delta\text{-}\mathrm{M(bpy)_3}][\Delta\text{-}\mathrm{Li}\Delta\text{-}\mathrm{Cr(ox)_3}] + \Lambda\text{-}[\mathrm{Cr(ox)_3}]^{3-}$$

$$\Lambda\text{-}[\mathrm{M(bpy)_3}]^{2+} + 2\,(rac)\text{-}[\mathrm{Cr(ox)_3}]^{3-} + \mathrm{Li}^{+} = [\Lambda\text{-}\mathrm{M(bpy)_3}][\Lambda\text{-}\mathrm{Li}\Delta\text{-}\mathrm{Cr(ox)_3}] + \Lambda\text{-}[\mathrm{Cr(ox)_3}]^{3-}$$

The advantage of this method becomes obvious when ruthenium(II) complexes are used. The inertness of these d^6 low-spin complexes implies a remarkable configurational stability of the resolved complexes. Through enantioselective self-assembly, they can thus be used to obtain optically active compounds with a total control of the configuration of all the tris(chelated) metal centres of the material. Optically active 3D compounds have been obtained starting from resolved $[\mathrm{Ru(bpy)_3}]^{2+}$ combined with free oxalate and “naked” metal ions as powders [6,24] as described in the following reaction:

$$\Delta\text{-}[\mathrm{Ru(bpy)_3}]^{2+} + 3\mathrm{ox}^{2-} + 2\mathrm{Cu}^{2+} = [\Delta\text{-}\mathrm{Ru(bpy)_3}][\Delta\text{-}\mathrm{Cu_2(ox)_3}]$$

This strategy has been pursued to obtain optically active single crystals of $[\Delta\text{-}\mathrm{Ru(bpy)_3}][\Delta\text{-}\mathrm{Mn_2(ox)_3}]$ and $[\Lambda\text{-}\mathrm{Ru(bpy)_3}][\Lambda\text{-}\mathrm{Mn_2(ox)_3}]$. Using resolved $[\mathrm{Ru(bpy)_2(ppy)}]^{+}$, it was possible to obtain the 3D optically active ferromagnet $[\Delta\text{-}\mathrm{Ru(bpy)_2(ppy)}][\Delta\text{-}\mathrm{Mn}\Delta\text{-}\mathrm{Cr(ox)_3}]$ and $[\Lambda\text{-}\mathrm{Ru(bpy)_2(ppy)}][\Lambda\text{-}\mathrm{Mn}\Lambda\text{-}\mathrm{Cr(ox)_3}]$ as single crystals [6].

4. Two-dimensional bimetallic networks

4.1. Heterochirality and bidimensionality

As 3D compounds are composed of tris(chelated) bridged metal complexes and are the result of the association of homochiral moieties, their 2D analogues result from a heterochiral

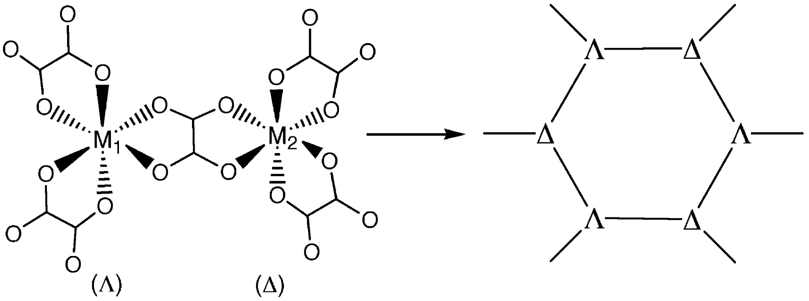

Fig. 6. Heterochiral arrangement of the neighbouring tris(chelated) metal centres leads to a 2D (6,3) anionic network.

arrangement of such moieties in which adjacent propeller-like chiral elements have opposite configurations (Fig. 6). This simple statement has many consequences.

Let us consider a single $[\Delta\text{-M}_1\Lambda\text{-M}_2(\text{ox})_3]^{n-}$ (6,3) honeycomb anionic layer. If the metal ions are identical – a situation never experimentally encountered – , the chirality of this layer merely vanishes. Going back to real compounds, following Avnir's quantitative approach of chirality [8], this means that a heterometallic 2D (6,3) anionic layer is less chiral that its helical 3D (10,3) analogue. An experimental consequence of this situation is that a long-range order sensitive technique like X-ray diffraction is able to detect the chirality of the anionic layer only if the M_i–O ($i = 1,2$) distances are significantly different from one another.

Upon this problem concerning one anionic layer, a difficulty associated with layer stacking is superimposed. $A[MnCr(ox)_3]$ ($A = NR_4$ ($R = Pr, Bu$), PPh_4) crystallises in the $R3c$ space group. The unit cell contains six anionic layers. Adjacent layers correspond to one another through a gliding mirror which inverts the configuration of each metal ion, i.e. a $[\Delta\text{-Mn}\Lambda\text{-Cr(ox)}_3]^-$ leads to a $[\Lambda\text{-Mn}\Delta\text{-Cr(ox)}_3]^-$ neighbouring layer, rendering the overall structure achiral (Fig. 7a).

On the contrary, $NBu_4[FeCr(ox)_3]$ crystallises in the $P6_3$ space group [31]. The unit cell, contrary to six-layered achiral $R3c$ structure, contains only two layers. In this space group, adjacent layers correspond to one another through the 6_3 screw axis which preserves the configuration of each metal ion, i.e. a $[\Delta\text{-Mn}\Lambda\text{-Cr(ox)}_3]^-$ leads to a $[\Delta\text{-Mn}\Lambda\text{-Cr(ox)}_3]^-$ neighbouring layer (Fig. 7b). Because the $R3c$ and $P6_3$ compounds only differ by the organisation of the layers, the $(h\,k\,0)$ diffraction peaks associated with the organisation within the layers themselves, are identical. The differences in the diffraction patterns are then not so obvious and the overall chirality of these 2D compounds has sometimes been neglected.

The second consequence of the "weak" chirality of the 2D compounds is that, compared to 3D compounds, the pathway towards enantioselective self-assembly, if existing, is not straightforward. The existence of an enantiospecific interaction between the cationic counterpart and the anionic layer is questionable. It is partly answered by analysing the available single crystal structures. The described cases of spontaneous resolution must be analysed to discern whether it might be possible to perform cation-driven enantioselective self-assembly of 2D (6,3) compounds.

The 2D compound $PPh_4[MnCr(ox)_3]$ crystallises in the $R3c$ space group [17,36]. The $[MnCr(ox)_3]^-$ adopts the classical honeycomb structure. The tetraphenylphosphonium cation stands between the layers. The P–C bond perpendicular to the anionic layer is located on the three-fold axis. The angle between the three remaining phenyl groups and the anionic layer is 52°. Because it is different from 0° or 90°, the phosphonium cation itself adopts a propeller-like chirality and its point group is D_3 regardless of the disordered perpendicular phenyl group. The existence of the gliding mirror as a symmetry operation of the

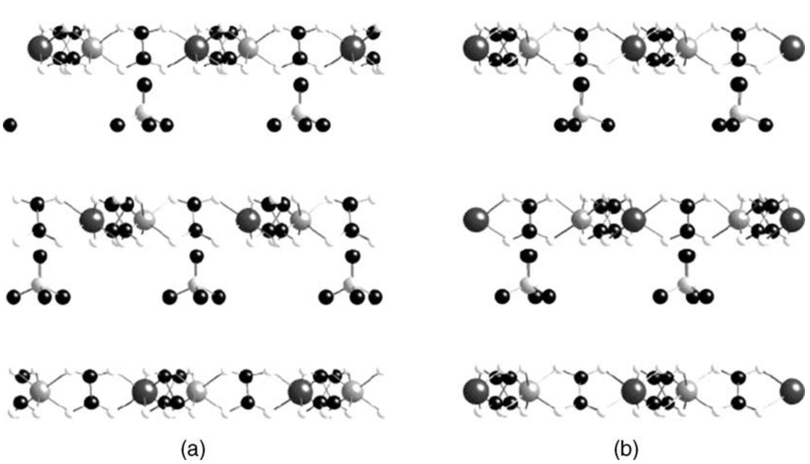
(a)
(b)

Fig. 7. Honeycomb layers stacking for 2D compounds crystallising in the $R3c$ achiral space group (a) and in the $P6_3$ chiral space group (b). In sake of clarity, only the four first carbon atoms of the alkyl chains around the nitrogen atom of the $[N(n\text{-}C_4H_9)_4]^+$ cation are shown (taken from Ref. [31]).

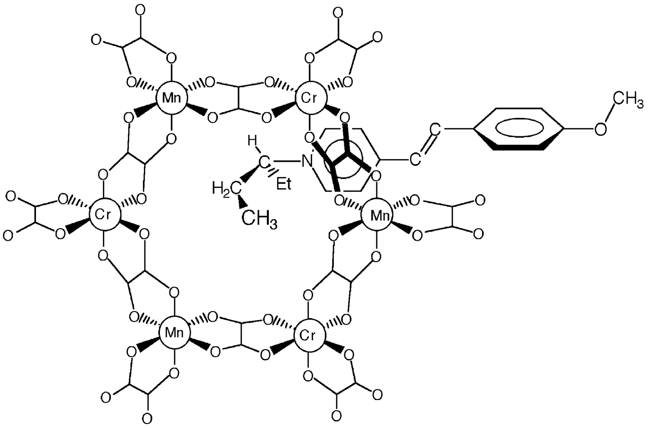

Fig. 8. (*R*,Λ) MIPS cation associated with a [Λ–MnΔ–Cr]$^-$ anionic layer (taken from Ref. [42]).

*R*3*c* space group implies that the rotation of the three equatorial phenyl groups around their C–P bound is alternatively clockwise and anti-clockwise, i.e. the two enantiomers exist in the compound. Recalling that each phosphonium cation stands just above a "Cr$(ox)_3$" moiety of the underlying layer, it is interesting to establish the relative configurations between these two chiral elements. It is found as (Δ,Λ) or (Δ,Λ) contrasting with the homochiral arrangement found in the 3D compound $[PPh_3Me][NaCr(ox)_3]$ [20]. Through this analysis, it appears that the tris(oxalato)metalate moiety can act as a chiral inductor within these compounds, so that achiral cations acquire a chiral conformation.

Among the stilbazolium cations introduced in 2D oxalate-based compounds in order to synthesise materials combining NLO and magnetism, special attention is paid to the monoclinic crystal structure of MIPS$[MnCr(ox)_3]$ (MIPS = 4-[4-methoxy-α-styryl]-*N*-isopentylpyridinium) [34]. This belongs to the $P2_1/c$ achiral space group. When associated with an iodide counter-anion, the MIPS cation is planar and thus achiral [42] while it has a twisted conformation when located in a layered $[MnCr(ox)_3]^-$ matrix [34]. In the latter case, the dihedral angle between the benzene and pyridinium ring is as large as 30.8°. From this twisting arises a helical chirality of the cation whose conformations can be labelled as (Δ) and (Λ). Moreover the MIPS cation interacts with the $[MnCr(ox)_3]^-$ anionic honeycomb layer through one of the ethyl chains of the *N*-isopentyl group (Fig. 8). These chains actually occupy two different positions. One is parallel to the anionic layers while the other penetrates one cell of the honeycomb layer. The van der Waals interactions with the anionic layer are thus different for the two ethyl chains linked to the carbon atom bounded to the nitrogen atom. This prochiral carbon atom thus becomes chiral. Because MIPS$[MnCr(ox)_3]$, described by Bénard et al. [34], was obtained starting from racemic tris(oxalato)chromate(III), both configurations of the metal ions are present in the compound as well as both chiral conformers of the MIPS cation. A careful analysis of the structure of the achiral MIPS$[MnCr(ox)_3]$ compound shows that the MIPS cation interacting with a [Λ-MnΔ-Cr$(ox)_3]^-$ anionic layer adopts the (*R*,Λ) configuration while (*S*,Δ)-MIPS is associated with a [Δ-MnΛ-Cr$(ox)_3]^-$ anionic layer, revealing specific interactions between the chiral anionic layer and the MIPS cation.

Through these two examples, the $[MnCr(ox)_3]^-$ matrix appears to be able to behave as a chiral inductor towards initially achiral counter-ions.

4.2. *Spontaneous resolution*

$NPn_4[MnFe(ox)_3]$ (Pn = *n*-C_5H_{11}) was reported to crystallise in the chiral $C222_1$ space group [43]. The elongation of alkyl chain by a single CH_2 group causes a drastic lowering of crystal symmetry from trigonal *R*3*c* to rhombic $C222_1$ space group.

This chiral space group surprised the authors themselves because it implies that the self-assembly process with the *symmetric* template $[NPn_4]^+$ cation occurs with spontaneous resolution. This led to a systematic study undertaken on single crystals that confirmed the initially reported crystallographic data [44]. The interpretation of this evolution towards chiral crystallites when going from tetrabutyl to tetrapentyl ammonium proposed by Shilov et al. can be summed up as follows:

(i) Due to its longer alkyl chains, $[NPn_4]^+$ cation has a "laying" position that differs from the "standing" position of $[NBu_4]^+$ leading to the loss of the three-fold axis. The local symmetry is lowered to two-fold. Two pentyl chains are now nearly parallel to the anionic layers while the two others are imbedded into hexagonal cells of upper and lower anionic layers, respectively.
(ii) As described in the case of the MIPS cation, due to the intermolecular interactions between these "embedded" alkyl chains and the anionic layers, the cation loses the S_4 symmetry operations existing in the regular tetrahedral conformation and acquires a chiral conformation (C_2 point group).
(iii) The symmetry driven specific interactions of terminal methyl groups with oxygen atoms of the oxalate groups of neighbouring layers leads to a homochiral configuration of the anionic layers.

This example proves the existence of 2D chiral networks when starting from an achiral cation and racemic tris(oxalato)metallates. Note that once again the spontaneous resolution and chiral space group does not lead to optical activity of the bulk crystalline material. Even the $NPn_4[MnFe(ox)_3]$ single crystals were found to be racemic twins, i.e. composed of chiral crystalline domains of opposite configurations.

Another example of spontaneous resolution is given by using an achiral member of the stilbazolium family, namely 4-[4-(dimethylamino)-phenylazo]-1-methylpyridinium (DAZOP) [45].

4.3. *Enantioselective self-assembly of powdered samples*

The enantiospecific supramolecular interactions between the cationic counterpart and the 2D anionic network are well-established by the above examples but, in contrast with the situation encountered in the 3D compounds, the variety of the template cations makes it difficult to figure out the best way towards enantioselective self-assembly.

The first strategy described for 3D compounds based on an anionic brick configurational control is still valid for 2D compounds. The absolute configuration of the "$M^{III}(ox)_3$" in the 2D network is ruled by the absolute configuration of starting anionic resolved building blocks if it does not racemise faster than the self-assembly takes place.

Starting from resolved tris(oxalato)chromate(III), $NBu_4[Mn\Delta\text{-}Cr(ox)_3]$ and $NBu_4[Mn\Lambda\text{-}Cr(ox)_3]$ were obtained as crystalline powders. They were found to belong to the chiral $P6_3$ space group while the space group is $R3c$ for powders synthesised from (*rac*)-$[Cr(ox)_3]^{3-}$ [46].

In the $P6_3$ space group, the symmetry operation transforming one cation into another is no longer a gliding mirror but a 6_3 screw axis (Fig. 3b). As exemplified in the case of PPh_4 cation in $PPh_4[MnCr(ox)_3]$, all the NBu_4 cations adopt the same chiral conformation. Nevertheless the disorder of the three alkyl chains of the tetrabutylammonium lying in the interlayer space prevents any further interpretation concerning a possible chiral conformation of this cation. Centered chiral quaternary ammonium salts $NR_1R_2R_3R_4^+$ have therefore been proposed to synthesise 2D bimetallic networks [30,31]. $[NEtPrBuPn]^+$ (Et = C_2H_5, Pr = *n*-C_3H_7), named N2345, was used to template the formation of 2D N2345$[MnCr(ox)_3]$ and N2345$[FeCr(ox)_3]$ using racemic or resolved $[Cr(ox)_3]^{3-}$, and N2345$[MnFe(ox)_3]$ starting from racemic $[Fe(ox)_3]^{3-}$. The first consequence of using the N2345 cation was an improved crystallinity of the sample compared to the symmetrical tetraalkyl ammonium analogues.

The experimental X-ray powder diffraction patterns for N2345$[MnCr(ox)_3]$ and N2345$[MnFe(ox)_3]$ obtained from racemic $[Cr(ox)_3]^{3-}$ as well as the single-crystal X-ray diffraction data obtained on N2345$[MnCr(ox)_3]$ were refined in the trigonal $R3c$ space group [31]. This result, identical to that obtained with symmetrical NBu_4 and NPr_4 cations, indicates that the cation displays disorder around the three-fold axis which is materialised by the axial butyl chain. This disorder prevents, if existing, a definitive determination of the configuration of the chiral ammonium-"$Cr(ox)_3$" moiety pairs. In contrast with Mn(II), Fe(II) combined with N2345 and (*rac*)-$[Cr(ox)_3]^{3-}$ led to a spontaneous resolution of the final 2D compound whose X-ray powder diffraction pattern has been refined in the chiral $P6_3$ space group.

As expected, starting from resolved Δ- or Λ-$[Cr(ox)_3]^{3-}$, both N2345$[MnCr(ox)_3]$ and N2345$[FeCr(ox)_3]$ led to pure $P6_3$ phases (following Nuttall and Day [47], peaks corresponding to the $R3c$ space group were attributed to stacking faults). Apart from the fact that their resolution process is not known, the disorder of the alkyl chains around the three-fold axis makes it unlikely that these nitrogen centred chiral ammonium ions can be used for enantioselective self-assembly of chiral 2D oxalate-based networks.

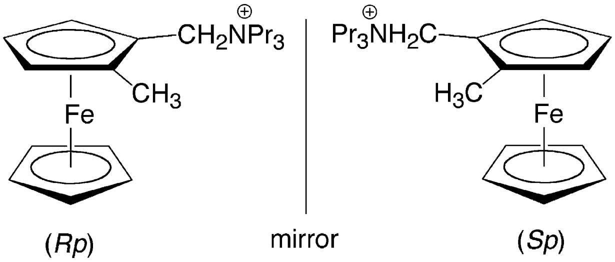

Fig. 9. Schematic representation of the (*Rp*) and (*Sp*) planar chiral 1-(*N*,*N*,*N*-tri(propyl)aminomethyl)-2-methylferrocene.

The synthesis of optically active stilbazolium containing 2D networks starting from resolved tris(oxalato)metalate has been undertaken. The correlation of the UV–vis properties of these networks with their natural circular dichroism (NDC) led to the conclusion that, in accordance with the enantiospecific interactions described in the structure obtained from (*rac*)-$[Cr(ox)_3]^{3-}$, the stilbazolium cations may become chiral in $[Mn^{II}Cr^{III}(ox)_3]^-$ anionic matrices and exhibit a dichroic signal and hence an absolute configuration, that depends on the configuration of the starting anionic reagent [42].

The above results clearly establish that the existence of enantiospecific interactions can be exploited to obtain optically active compounds using resolved counter cations as chiral templating agents.

Ferrocenyl substituted ammonium ions have been shown to be efficient template cations of 2D oxalate-based networks [48]. The planar chiral 1-(*N*,*N*,*N*-tri(alkyl)aminomethyl)-2-methylferrocene $[1\text{-}CH_2NR_3\text{-}2\text{-}CH_3\text{-}C_5H_3Fe\text{-}C_5H_5]^+$ (R = CH_3, *n*-C_2H_5, *n*-C_3H_7, *n*-C_4H_9) cations (Fig. 9), so-named (alkyl sub-

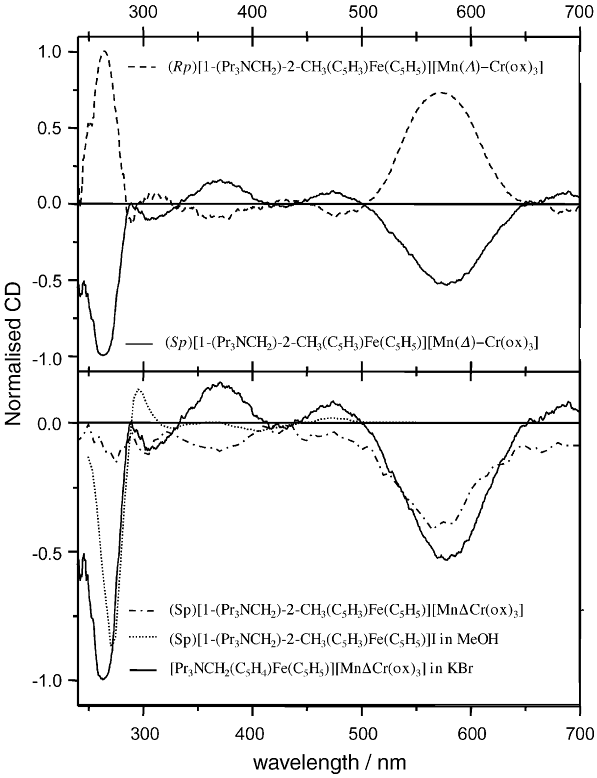

Fig. 10. Natural circular dichroism curves for compounds [(*Rp*),(Λ)]- and [(*Sp*),(Δ)]-$[(C_5H_5)Fe(C_5H_3)(CH_3)CH_2N(C_3H_7)_3][MnCr(C_2O_4)_3]$ in KBr pellets (a) [(*Sp*),(Δ)]-$[(C_5H_5)Fe(C_5H_3)(CH_3)CH_2N(C_3H_7)_3][MnCr(C_2O_4)_3]$, $[(C_5H_5)Fe(C_5H_4)CH_2N(C_3H_7)_3][Mn\,(\Delta)\text{-}Cr(C_2O_4)_3]$ in KBr pellets and (*Sp*)-$[(C_5H_5)Fe(C_5H_3)(CH_3)CH_2N(C_3H_7)_3]I$ in MeOH (b) (taken from Ref. [49]).

stituted) ferrocenic ammonium ions, associated with D_3 anions form diastereostereomeric ion pairs in solution [49]. Their resolved (*Rp*) or (*Sp*) iodide salts were thus tentatively used to template the enantioselective formation of 2D networks starting from (*rac*)-$[Cr(ox)_3]^{3-}$.

2D networks were obtained for R = Et and Pr. A dramatic difference is observed for the networks obtained from the ethyl and the propyl substituted optically active ferrocenic ammonium ions. For R = Et, the resulting 2D networks do not exhibit the dichroic signal corresponding with the d–d transition of the chromium(III) moiety while the propyl derivatives do (Fig. 10). In the latter case, determination of the relative configurations thanks to the sign of the dichroic signals led to the conclusion that the (*Rp*)-$[1\text{-}CH_2NR_3\text{-}2\text{-}CH_3\text{-}C_5H_3Fe\text{-}C_5H_5][Mn\Lambda\text{-}Cr(ox)_3]$ and (*Sp*)-$[1\text{-}CH_2NR_3\text{-}2\text{-}CH_3\text{-}C_5H_3Fe\text{-}C_5H_5][Mn\Delta\text{-}Cr(ox)_3]$ are enantioselectively obtained starting from (*Rp*) or (*Sp*)-$[1\text{-}CH_2N(n\text{-}C_3H_7)_3\text{-}2\text{-}CH_3\text{-}C_5H_3Fe\text{-}C_5H_5]^+$ respectively (Fig. 10) [49].

Naturally, the single crystal growth of these compounds was undertaken starting from the resolved (*Rp*)-$[1\text{-}CH_2N(n\text{-}C_3H_7)_3\text{-}2\text{-}CH_3\text{-}C_5H_3Fe\text{-}C_5H_5]^+$ cation and (*rac*)-$[Cr(ox)_3]^{3-}$ [50]. A $NHPr_3[MnCr(ox)_3]$ single crystal was obtained [50]. Its structure was refined in the $P6_3$ chiral space group. The formation of these $NHPr_3[MnCr(ox)_3]$ chiral single crystals is interpreted by a slow hydrolysis of the starting ammonium ion during the lengthy crystallisation process.

5. Summary

The structures of 3D and 2D oxalate-based compounds have been described. The control over dimensionality has been stressed by analysing new examples. It appears that the orientation towards 3D compounds using D_3 tris(diimine)metal complexes is valid only if all the metal ions of the anionic network are tris(chelated). Moreover non-D_3 cations have been successfully used to template the formation of 3D compounds thanks to supramolecular interactions between the counter-cations themselves.

The control of absolute configuration of 3D tris(chelated) oxalate-based compounds has been readily achieved relying on the obvious enantioselective interaction between the D_3 "$M(ox)_3$" moiety and the D_3 tris(diimine)metal complexes starting either from resolved tris(oxalato)metalate(III) or resolved tris(diimine)metal complexes. In the latter case, it is possible to perform enantioselective crystallisation of the material.

For 2D tris(chelated) oxalate-based compounds, due to the heterochirality of the adjacent metal centres within the layers as well as layer stacking, the problem appears much more complicated. The first step was to demonstrate that "$M(ox)_3$" moiety behaves as a chiral inductor towards an achiral template cation, leading to chiral conformation of the latter. It then has been shown that resolved ferrocenic ammonium ions were able to template the formation of optically active 2D powdered compounds. The next breakthrough will definitely come from the discovery of the chiral cation adapted to the enantioselective crystallisation of optically active 2D oxalate-based magnets.

Acknowledgements

This work was supported by the University Pierre et Marie Curie, CNRS and Russian Academy of Sciences (Program of Academician R. Sagdeev) and by the RFBR Grant No. 05-03-33026. The authors acknowledge the funding from CNRS/RAS Joint Research Program (Project No. 16332) and DFG Schwerpunktprogramm "Molekularer Magnetismus" (SPP 1137).

References

[1] D. Vivien, F. Mougel, G. Aka, A. Kahn-Harari, D. Pelenc, Laser Phys. 8 (1998) 759;
M.E. Itkis, X. Chi, A.W. Cordes, R.C. Haddon, Science 296 (2002) 1443;
I. Stamatin, A. Morozan, A. Dumitru, V. S., Fullerenes nanotubes and carbon nanostructures 13 (2005) 543.

[2] S. Decurtins, R. Pellaux, G. Antorrena, F. Palacio, Coord. Chem. Rev. (1999) 841.

[3] R. Clement, S. Decurtins, M. Gruselle, C. Train, in: W. Linert, M. Verdaguer (Eds.), Molecular Magnets: Recent Highlights, Springer, Wien, New York, 2003, p. 1.

[4] G.L.J.A. Rikken, E. Raupach, Phys. Rev. E 58 (1998) 5081;
G.L.J.A. Rikken, E. Raupach, Nature 390 (1997) 493.

[5] K. Inoue, K. Kikuchi, M. Ohba, H. Okawa, Angew. Chem., Int. Ed. 42 (2003) 4810;
E. Coronado, C. Gimenez-Saiz, J.M. Martinez-Agudo, A. Nuez, F.M. Romero, H. Stoeckli-Evans, Polyhedron 22 (2003) 2435.

[6] R. Andres, M. Brissard, M. Gruselle, C. Train, J. Vaissermann, B. Malezieux, J.-P. Jamet, M. Verdaguer, Inorg. Chem. 40 (2001) 4633.

[7] O. Kahn, Molecular Magnetism, Wiley–VCH Verlag GmbH, Weinheim, Germany, 1993;
S. Ferlay, T. Mallah, R. Ouahes, P. Veillet, M. Verdaguer, Nature 378 (1995) 701;
P. Yu, Y. Journaux, O. Kahn, Inorg. Chem. 28 (1989) 100;
M. Verdaguer, A. Bleuzen, V. Marvaud, J. Vaissermann, M. Seuleiman, C. Desplanches, A. Scuiller, C. Train, R. Garde, G. Gelly, C. Lomenech, I. Rosenman, P. Veillet, C. Cartier, F. Villain, Coord. Chem. Rev. 190–192 (1999) 1023.

[8] S. Alvarez, M. Pinsky, D. Avnir, Eur. J. Inorg. Chem. (2001) 1499;
S. Alvarez, M. Pinsky, M. Llunell, D. Avnir, Cryst. Eng. 4 (2001) 179;
S. Alvarez, P. Alemany, D. Avnir, Chem. Soc. Rev. 34 (2005) 313;
S. Alvarez, P. Alemany, D. Casanova, J. Cirera, M. Llunell, D. Avnir, Coord. Chem. Rev. 249 (2005) 1693.

[9] A. Von Zelewsky, O. Mamula, J. Chem. Soc., Dalton Trans. (2000) 219.

[10] J.S. Seo, D. Whang, H. Lee, S.I. Jun, J. Oh, J.Y. Jin, K. Kim, Nature 404 (2000) 982.

[11] J. Jean, A. Collet, S.H. Wilen, Enantiomers, Racemates and Resolutions, John Wiley edition, 1981.

[12] H. Tamaki, Z.J. Zhong, N. Matsumoto, S. Kida, M. Koikawa, N. Achiwa, Y. Hashimoto, H. Okawa, J. Am. Chem. Soc. 114 (1992) 6974.

[13] H. Tamaki, M. Mitsumi, K. Nakamura, N. Matsumoto, S. Kida, H. Okawa, S. Iijima, Mol. Cryst. Liq. Cryst. 233 (1993) 257.

[14] L.O. Atovmyan, G.V. Shilov, R.N. Lubovskaya, E.I. Zhilyaeva, N.S. Ovanesyan, S.I. Pirumova, I.G. Gusakovskaya, Y.G. Morozov, JETP Lett. 58 (1993) 766.

[15] S. Decurtins, H.W. Schmalle, P. Schneuwly, J. Ensling, P. Guetlich, J. Am. Chem. Soc. 116 (1994) 9521.

[16] P. Day, J. Chem. Soc., Dalton Trans. (1997) 701;
M. Hernandez-Molina, F. Lloret, C. Ruiz-Perez, M. Julve, Inorg. Chem. 37 (1998) 4131;
E. Coronado, J.R. Galan-Mascaros, C.J. Gomez-Garcia, J.M. Martinez-Agudo, Adv. Mater. 11 (1999) 558.

[17] S. Decurtins, H.W. Schmalle, H.R. Oswald, A. Linden, J. Ensling, P. Guetlich, A. Hauser, Inorg. Chim. Acta 216 (1994) 65.

[18] L.O. Atovmyan, G.V. Shilov, N.S. Ovanesyan, A.A. Pyalling, R.N. Lyubovskaya, E.I. Zhilyaeva, Y.G. Morozov, Synth. Met. 71 (1809).
[19] M. Pilkington, S. Decurtins, in: J.S. Miller, M. Drillon (Eds.), Magnetism: Molecules to Materials II, Wiley–VCH Verlag GmbH, Weinheim, Germany, 2001, p. 339.
[20] V.M. Russell, D.C. Craig, M.L. Scudder, I.G. Dance, CrystEngCommun 3 (2000) 1.
[21] D. Armentano, G. De Munno, M. Julve, F. lloret, Proceedings of the VIIth International Conference on Molecule-based Magnets, ICMM'2002 Valencia, Spain, 5–10 October 2002.
[22] D. Armentano, G. De Munno, F. Lloret, M. Julve, CrystEngCommun 7 (2005) 57.
[23] A. Alberola, E. Coronado, C. Gimenez-Saiz, C.J. Gomez-Garcia, F.M. Romero, A. Tarazon, Eur. J. Inorg. Chem. (2005) 389.
[24] F. Pointillart, C. Train, M. Gruselle, F. Villain, H.W. Schmalle, D. Talbot, P. Gredin, S. Decurtins, M. Verdaguer, Chem. Mater. 16 (2004) 832.
[25] C. Mathoniere, C.J. Nuttall, S.G. Carling, P. Day, Inorg. Chem. 35 (1996) 1201.
[26] E. Coronado, J.R. Galan-Mascaros, C.J. Gomez-Garcia, J.M. Martinez-Agudo, Inorg. Chem. 40 (2001) 113.
[27] E.C. Constable, J.M. Holmes, J. Organomet. Chem. 301 (1986) 203.
[28] M. Brissard, Université Pierre et Marie Curie, Paris, France, 2002.
[29] H.W. Schmalle, R. Pellaux, S. Decurtins, Z. Kristallogr. 211 (1996) 533.
[30] M. Gruselle, B. Malezieux, C. Train, C. Soulie, N. Ovanesyan, CR Chim. 6 (2003) 189.
[31] N.S. Ovanesyan, V.D. Makhaev, S.M. Aldoshin, P. Gredin, K. Boubekeur, C. Train, M. Gruselle, J. Chem. Soc., Dalton Trans. (2005) 3101.
[32] M. Clemente-Léon, E. Coronado, J.R. Galan-Mascaros, C.J. Gomez-Garcia, J. Chem. Soc., Chem. Commun. (1997) 1727.
[33] S. Bénard, E. Rivière, P. Yu, K. Nakatani, J.-F. Delouis, Chem. Mater. 13 (2000) 159.
[34] S. Bénard, P. Yu, J.P. Audière, E. Rivière, R. Clément, J. Guilhem, L. Tchertanov, K. Nakatani, J. Am. Chem. Soc. 122 (2000) 9444.
[35] E. Coronado, J.R. Galan-Mascaros, C.J. Gomez-Garcia, V. Laukhin, Nature 408 (2000) 447.
[36] G.V. Shilov, L.O. Atovmyan, N.S. Ovanesyan, A.A. Pyalling, L. Bottyan, Russ. J. Coord. Chem. 24 (1995) 288.
[37] G.V. Shilov, N.S. Ovanesyan, N.A. Sanina, A.A. Pyalling, L.O. Atovmyan, Russ. J. Coord. Chem. 24 (1998) 802;
I.D. Watts, S.G. Carling, P. Day, J. Chem. Soc., Dalton Trans. (2002) 1429.
[38] I. Hargittai, M. Hargittai, Symmetry Through the Eyes of a Chemist, 2nd ed., Plenum Press, New York, 1995.
[39] R. Andres, M. Gruselle, B. Malezieux, M. Verdaguer, J. Vaissermann, Inorg. Chem. 38 (1999) 4637.
[40] H.D. Flack, G. Bernardinelli, Acta Cryst. A 55 (1999) 908;
H.D. Flack, G. Bernardinelli, J. Appl. Crystallogr. 33 (2000) 1143.
[41] M. Brissard, H. Amouri, M. Gruselle, R. Thouvenot, CR Chim. 5 (2002) 53.
[42] M. Gruselle, B. Malezieux, S. Benard, C. Train, C. Guyard-Duhayon, P. Gredin, K. Tonsuaadu, R. Clement, Tetrahedron: Asymmetry 15 (2004) 3103.
[43] S.G. Carling, C. Mathoniere, P. Day, K.M.A. Malik, S.J. Coles, M.B. Hursthouse, J. Chem. Soc., Dalton Trans. 1996 (1839).
[44] G.V. Shilov, N.S. Ovanesyan, N.A. Sanina, L.O. Atovmyan, M. Gruselle, Russ. J. Coord. Chem. 27 (2001) 567.
[45] J.S.O. Evans, S. Benard, P. Yu, R. Clement, Chem. Mater. 13 (2001) 3813;
P.G. Lacroix, I. Malfant, S. Benard, P. Yu, E. Riviere, K. Nakatani, Chem. Mater. 13 (2001) 441.
[46] N.S. Ovanesyan, G.V. Shilov, A.A. Pyalling, C. Train, P. Gredin, M. Gruselle, L.F. Kiss, L. Bottyan, J. Magn. Magn. Mater. 272–276 (2004) 1089.
[47] C.J. Nuttall, P. Day, J. Solid State Chem. 147 (1999) 3.
[48] B. Malezieux, R. Andres, M. Brissard, M. Gruselle, C. Train, P. Herson, L.L. Troitskaya, V.I. Sokolov, S.T. Ovseenko, T.V. Demeschik, N.S. Ovanesyan, I.A. Mamed'yarova, J. Organomet. Chem. 637–639 (2001) 182.
[49] M. Gruselle, R. Thouvenot, B. Malezieux, C. Train, P. Gredin, T.V. Demeschik, L.L. Troitskaya, V.I. Sokolov, Chem. Eur. J. 10 (2004) 4763.
[50] G.V. Shilov, N.S. Ovanesyan, S.M. Aldoshin, M. Gruselle, C. Train, C. Guyard-Duhayon, J. Coord. Chem. 57 (2004) 1165.